Development and Verification of an Orthotropic Elasto-Plastic Three-Dimensional Model with Tabulated Input Suitable for Use in Composite Impact Problems

Robert K. Goldberg
NASA Glenn Research Center, Cleveland OH
Kelly S. Carney and Paul DuBois
George Mason University, Fairfax VA
Bilal Khaled, Loukham Shymasunder, Canio Hoffarth and Subramaniam Rajan
Arizona State University, Tempe AZ
Gunther Blankenhorn
Livermore Software Technology Corporation, Livermore CA

Abstract

A material model which incorporates several key capabilities which have been identified by the aerospace community as lacking in the composite impact models currently available in LS-DYNA® is under development. In particular, the material model, which is being implemented as MAT 213 into a tailored version of LS-DYNA being jointly developed by the FAA and NASA, incorporates both plasticity and damage within the material model and utilizes experimentally based tabulated input to define the evolution of plasticity and damage as opposed to specifying discrete input parameters (such as modulus and strength. The plasticity portion of the orthotropic, three-dimensional, macroscopic composite constitutive model is based on an extension of the Tsai-Wu composite failure model into a generalized yield function with a non-associative flow rule. The capability to account for the rate and temperature dependent deformation response of composites has also been incorporated into the material model. For the damage model, a strain equivalent formulation is utilized to allow for the uncoupling of the deformation and damage analyses. In the damage model, a diagonal damage tensor is defined to account for the directionally dependent variation of damage. However, the terms in the damage matrix are semi-coupled such that the damage in a particular coordinate direction is a function of the stresses and plastic strains in all of the coordinate directions. For the failure model, a tabulated approach is utilized in which a stress or strain based invariant is defined as a function of the location of the current stress state in stress space to define the initiation of failure, which allows an arbitrarily shaped failure surface to be defined. A wide ranging series of verification studies on a variety of composite systems has been carried out.

Introduction

As composite materials are gaining increased use in aircraft components where impact resistance is critical (such as the turbine engine fan case), the need for accurate material models to simulate the deformation, damage and failure response of polymer matrix composites under impact conditions is gaining in importance. While there are several material models currently available within commercial transient dynamic codes such as LS-DYNA [1] to analyze the impact response of composites, areas have been identified where the predictive capabilities of these models can be improved. Most importantly, the existing models often require extensive correlation based on structural level impact tests, which significantly limits the ability to use these models as predictive tools. Furthermore, most of the existing models apply either a plasticity based approach (such as that used by Sun and Chen [2]) or a continuum damage mechanics approach (such as that used by Matzenmiller et al [3]) to simulate the nonlinearity that takes place in the composite response. As documented in detail by Goldberg, et al [4, 5], either of these approaches can capture certain aspects of the actual composite behavior. However, optimally, combining a plasticity based deformation model (to capture the rate dependence and

significant nonlinearity, particularly in shear, observed in the composite response) with a damage model (to account for the changes in the unloading modulus observed as the material is unloaded from various stress levels, as well as to account for strain softening observed after the peak stress is reached) can provide advantages over using one approach or the other. In addition, the input to current material models generally consists of point-wise properties (such as the modulus, failure stress or failure strain in a particular coordinate direction) that leads to curve fit approximations to the material stress-strain curves. This type of approach either leads to models with only a few parameters, which provide a crude approximation at best to the actual material response, or to models with many parameters which require a large number of complex tests to characterize. An improved approach is to use tabulated data, obtained from a well-defined set of straightforward experiments. Using tabulated data allows the actual material response data to be entered in discretized form, which permits a more accurate representation of the actual material response.

   To begin to address these needs, a new composite material model is being developed and implemented for use within LS-DYNA. The material model is being implemented as MAT 213. The material model is meant to be a fully generalized model suitable for use with any composite architecture (laminated or textile). The deformation model is based on extending the commonly used Tsai-Wu composite failure model [6] to a strain hardening plasticity model with a non-associative flow rule. For the damage model, a strain equivalent formulation is used in which the deformation and damage calculations can be uncoupled. A significant feature in the developed damage model is that a semi-coupled approach has been utilized in which a load in a particular coordinate direction results in damage (and thus stiffness reduction) in multiple coordinate directions. While different from the approach used in many existing damage mechanics models [3] in which a load in a particular coordinate direction only leads to a stiffness reduction in the load direction, this approach has the potential to more accurately reflect the damage behavior that actually takes place, particularly for composites with more complex fiber architectures.

   A wide variety of failure models, which mark the end of the stress-strain curve, have been developed for composites. In models such as the Tsai-Wu failure model [6], a quadratic function of the macroscopic stresses is defined in which the coefficients of the failure function are related to the tensile, compressive and shear failure stresses in the various coordinate directions. This model, while mathematically simple and easy to implement numerically, assumes that the composite failure surface has an ellipsoidal (in 2D) or ovoid (in 3D) shape. In reality, composite failure surfaces often are not in the form of simple shapes. More complex models, such as the Hashin model [7], also utilize quadratic combinations of the macroscopic failure stresses, but utilize only selective terms in the quadratic function in order to link the macroscopic stresses to local failure modes such as fiber or matrix failure. However, an overall quadratic form to the failure functions (albeit in a piecewise fashion) are still assumed. This approach was extended in models such as those developed by Puck et al. [8], Pinho et al. [9] and Maimi et al. [10], in which complex equations were developed to predict local failure mechanisms in terms of macroscopic level stresses. In this manner, the failure response and complex failure surfaces present in actual composites could be more accurately represented. However, in these advanced models, very complex tests are often required to characterize the model parameters and the applicability of the models may be limited to specific composite architectures with specific failure mechanisms. In a combination of approaches, researchers such as Mayes and Hansen [11] and Feng [12] utilize an approach where stress (or strain) invariants based on macroscopic stresses are used to define the initiation of failure. However, different forms of the invariants are used to determine whether fiber-dominated or matrix-dominated failure occurs. Given the variety of failure models present in the literature, activities such as the World Wide Failure Exercise and its multiple iterations (e.g. [13], [14], and [15]) have attempted to conduct a rigorous review of which failure model or models provides the optimum prediction of composite failure. In all of these studies, none of the examined models showed a complete ability to predict composite failure or displayed a significant advantage compared to the other models examined.

   The difficulty in simulating composite failure can be related to the fact that in reality failure is a highly localized phenomenon dependent on various combination of fiber, matrix and interface failures. Due to these complex and interacting local failure mechanisms, and the fact that these mechanisms can vary based on the

constituent materials and fiber architecture, in reality the actual composite failure surface often does not conform to a shape that can be easily simulated using a simple mathematical function. Conversely, attempts to utilize discrete functions to analyze the complex local mechanisms can result in models with a large number of parameters that require a highly complex test program to obtain. In the methodology described in this paper, an approach is used in which the actual experimental three-dimensional failure envelope for a composite is entered in a tabulated fashion. Specifically, a stress or strain based invariant leading to the initiation of failure is defined as a function of the location of the current stress state in stress space. In this manner, an arbitrary failure surface can be easily defined based on actual experimental data in combination with numerical data obtained using any desired existing failure model. The current approach thus serves as a general framework which is not limited to any arbitrarily imposed failure surface based on an arbitrarily defined mathematical function.

In the following sections of this paper, a brief summary of the plasticity-based deformation model is presented. The key aspects of the damage model and its characterization are then described. Details of the failure model are then discussed, including the overall methodology and a sample of how it can be applied for a particular composite. A detailed overview of the program that is being undertaken to verify and validate the MAT 213 material model will also be presented.

Deformation Model Overview

A complete description of the deformation model is given in Goldberg et al [4, 5]. A summary of the key features of the model is presented here. In the deformation model, a general quadratic three-dimensional orthotropic yield function based on the Tsai-Wu failure model is specified as follows, where 1, 2, and 3 refer to the principal material directions:

$$
f(\sigma) = -1 + \begin{pmatrix} F_1 & F_2 & F_3 & 0 & 0 & 0 \end{pmatrix} \begin{pmatrix} \sigma_{11} \\ \sigma_{22} \\ \sigma_{33} \\ \sigma_{12} \\ \sigma_{23} \\ \sigma_{31} \end{pmatrix}
$$

$$
+ \begin{pmatrix} \sigma_{11} & \sigma_{22} & \sigma_{33} & \sigma_{12} & \sigma_{23} & \sigma_{31} \end{pmatrix} \begin{pmatrix} F_{11} & F_{12} & F_{13} & 0 & 0 & 0 \\ F_{12} & F_{22} & F_{23} & 0 & 0 & 0 \\ F_{13} & F_{23} & F_{33} & 0 & 0 & 0 \\ 0 & 0 & 0 & F_{44} & 0 & 0 \\ 0 & 0 & 0 & 0 & F_{55} & 0 \\ 0 & 0 & 0 & 0 & 0 & F_{66} \end{pmatrix} \begin{pmatrix} \sigma_{11} \\ \sigma_{22} \\ \sigma_{33} \\ \sigma_{12} \\ \sigma_{23} \\ \sigma_{31} \end{pmatrix}
$$

(1)

In the yield function, σ_{ij} represents the stresses and F_{ij} and F_k are coefficients that evolve and are functions of the current values of the stresses in the various coordinate directions. By allowing the coefficients to vary, the yield surface evolution and hardening in each of the material directions can be precisely defined. The values of the normal and shear coefficients can be determined by simplifying the yield function for the case of unidirectional tensile and compressive loading in each of the coordinate directions along with shear tests in each of the shear directions. In the above equation, the stresses are the current value of the yield stresses in the normal and shear directions. To determine the values of the off-axis coefficients (which are required to capture the stress interaction effects), the results from 45° off-axis tests (an arbitrarily chosen angle) in the various coordinate directions can be used. The values of the off-diagonal terms in the yield function can also be modified as required in order to ensure that the yield surface is convex [5].

A non-associative flow rule is used to compute the evolution of the components of plastic strain. The plastic potential for the flow rule is shown in Equation (2) below:

$$h = \sqrt{H_{11}\sigma_{11}^2 + H_{22}\sigma_{22}^2 + H_{33}\sigma_{33}^2 + 2H_{12}\sigma_{11}\sigma_{22} + 2H_{23}\sigma_{22}\sigma_{33} + 2H_{31}\sigma_{33}\sigma_{11} + H_{44}\sigma_{12}^2 + H_{55}\sigma_{23}^2 + H_{66}\sigma_{31}^2}$$

(2)

where σ_{ij} are the current values of the stresses and H_{ij} are independent coefficients, which are assumed to remain constant. The values of the coefficients are computed based on average plastic Poisson's ratios [4, 5]. The plastic potential function in Equation (2) is used in a flow law to compute the components of the plastic strain rate, where the usual normality hypothesis from classical plasticity [16] is assumed to apply.

Given the flow law, the principal of the equivalence of plastic work [16] can be used to determine that the plastic potential function, *h*, can be defined as the effective stress and the plastic multiplier can be defined as the effective plastic strain rate.

To compute the current value of the yield stresses needed for the yield function, tabulated stress-strain curves are used to track the yield stress evolution. The user is required to input twelve stress versus plastic strain curves. Specifically, the required curves include uniaxial tension curves in each of the normal directions (1,2,3), uniaxial compression curves in each of the normal directions (1,2,3), shear stress-strain curves in each of the shear directions (1-2, 2-3 and 3-1), and 45 degree off-axis tension or compression curves in each of the 1-2, 2-3 and 3-1 planes. The 45 degree curves are required in order to properly capture the stress interaction effects. By utilizing tabulated stress-strain curves to track the evolution of the deformation response, the experimental stress-strain response of the material can be captured exactly without any curve fit approximations. The required stress-strain data can be obtained either from actual experimental test results or by appropriate numerical experiments utilizing stand-alone codes. The ability to account for rate and temperature effects has also been incorporated into the deformation model. To track the evolution of the deformation response along each of the stress-strain curves, the effective plastic strain is chosen to be the tracking parameter. Using a numerical procedure based on the radial return method [16] in combination with an iterative approach, the effective plastic strain is computed for each time/load step. The stresses for each of the tabulated input curves corresponding to the current value of the effective plastic strain are then used to compute the yield function coefficients.

Damage Model Overview

The deformation portion of the material model provides the majority of the capability of the model to simulate the nonlinear stress-strain response of the composite. However, in order to capture the changes in the unloading modulus observed as the material is unloaded from various stress levels and the local softening of the stress-strain response that is often observed in composites [17], a complementary damage law is required. Strain equivalence is assumed in the damage law formulation, therefore the total, elastic and plastic strains in the actual and effective stress spaces are the same for every time step [18]. The utilization of strain equivalence permits the plasticity and damage calculations to be uncoupled, as all of the plasticity computations can take place in the effective stress space.

The first step in the development of the damage model is to relate the actual stresses to a set of effective stresses by use of a damage tensor **M**. Given the usual assumption that the actual stress tensor and the effective stress tensor are symmetric, the actual stresses can be related to the effective stresses in the following manner, where the damage tensor **M** is assumed to have a maximum of 36 independent components:

$$\begin{pmatrix} \sigma_{11} \\ \sigma_{22} \\ \sigma_{33} \\ \sigma_{12} \\ \sigma_{23} \\ \sigma_{13} \end{pmatrix} = [\mathbf{M}] \begin{pmatrix} \sigma_{11}^{eff} \\ \sigma_{22}^{eff} \\ \sigma_{33}^{eff} \\ \sigma_{12}^{eff} \\ \sigma_{23}^{eff} \\ \sigma_{13}^{eff} \end{pmatrix} \qquad (3)$$

In order to maintain a one to one relationship between the effective stresses and the actual stresses (i.e. to ensure that a uniaxial load in the actual stress space does not result in a multi-axial load in the effective stress space), the damage tensor is assumed to be diagonal An implication of a diagonal damage tensor is that loading the composite in a particular coordinate direction only leads to a stiffness reduction in the direction of the load due to the formation of matrix cracks perpendicular to the direction of the load. However, as discussed in detail in Goldberg, et al. [5], in actual composites, particularly those with complex fiber architectures, a load in one coordinate direction can lead to stiffness reductions in multiple coordinate directions. To maintain a diagonal damage tensor while still allowing for the damage interaction in at least a semi-coupled sense, each term in the diagonal damage matrix should be a function of the plastic strains in each of the normal and shear coordinate directions, as follows for the example of the M_{11} term for the plane stress case:

$$M_{11} = M_{11}\left(\varepsilon_{11}^{p}, \varepsilon_{22}^{p}, \varepsilon_{12}^{p}\right) \qquad (4)$$

Note that plastic strains are chosen as the "tracking parameter" due to the fact that, within the context of the developed formulation, the material nonlinearity during loading is simulated by use of a plasticity based model. The plastic strains therefore track the current state of load and deformation in the material. To explain this concept of damage coupling further, assume a load is applied in the 1 direction to an undamaged specimen. The undamaged modulus in the 1-direction is E_{11} and the undamaged modulus in the 2-direction is E_{22}. The stress-strain response of the material is assumed to become nonlinear (represented in the current model by the accumulation of plastic strain) and damage is assumed to occur. The original specimen is unloaded and reloaded elastically in the 1-direction. Due to the damage, the reloaded specimen has a reduced modulus in the 1-direction of E_{11}^{d11}.   The reduced area and modulus are a function of the damage induced by the loading and resulting nonlinear deformation in the 1 direction (reflected as plastic strain) as follows:

$$E_{11}^{d11} = \left(1 - d_{11}^{11}\left(\varepsilon_{11}^{p}\right)\right)E_{11} \qquad (5)$$

where d_{11}^{11} is the damage in the 1-direction due to a load in the 1-direction.   Note that damage is only assumed to initiate once plastic strains have started to accumulate. Alternatively, if the damaged specimen was reloaded elastically in the 2-direction, due to the assumed damage coupling resulting from the load in the 1-direction, the reloaded specimen would have a reduced modulus in the 2-direction of E_{22}^{d11}. The reduced modulus is also a function of the damage induced by the load and resulting nonlinear deformation in the 1-direction as follows:

$$E_{22}^{d11} = \left(1 - d_{11}^{22}\left(\varepsilon_{11}^{p}\right)\right)E_{22} \qquad (6)$$

where d_{11}^{22} is the damage in the 2-direction due to a load in the 1-direction. Similar arguments can be made and equations developed for the situation where the original specimen is loaded in the 2-direction.

For the case of multiaxial loading, the semi-coupled formulation needs to account for the fact that as the load is applied in a particular coordinate direction, the loads are acting on damaged areas due to the loads in the other coordinate directions, and the load in a particular direction is just adding to the damaged area. For example, if one loaded the material in the 2-direction first, the reduced modulus in the 1-direction would be equal to E_{11}^{d22}. If one would then subsequently load the material in the 1-direction, the baseline modulus in the 1-direction would not be equal to the original modulus E_{11}, but instead the reduced modulus E_{11}^{d22}. These results suggest that the relation between the actual stress and the effective stress should be based on a multiplicative combination of the damage terms as opposed to an additive combination of the damage terms. For example, for the case of plane stress, the relation between the actual and effective stresses could be expressed as follows:

$$\sigma_{11} = \left(1 - d_{11}^{11}\right)\left(1 - d_{22}^{11}\right)\left(1 - d_{12}^{11}\right)\sigma_{11}^{eff}$$
$$\sigma_{22} = \left(1 - d_{11}^{22}\right)\left(1 - d_{22}^{22}\right)\left(1 - d_{12}^{22}\right)\sigma_{22}^{eff} \tag{7}$$
$$\sigma_{12} = \left(1 - d_{11}^{12}\right)\left(1 - d_{22}^{12}\right)\left(1 - d_{12}^{12}\right)\sigma_{12}^{eff}$$

where for each of the damage terms the subscript indicates the direction of the load which initiates the particular increment of damage and the superscript indicates the direction in which the damage takes place. For the full three-dimensional case the actual stresses would be functions of damage parameters in all six coordinate directions.

To properly characterize the damage model, an extensive set of test data is required. Due to the tabulated nature of the input, each of the damage parameters (d_{11}^{22}, d_{11}^{22}, etc.) has to be determined as a function of the plastic strain in a particular coordinate direction (such as ε_{11}^{p}). For example, to determine the damage terms for the case of loading in the 1-direction, a composite specimen has to be loaded to a certain plastic strain level in the 1-direction. The material is then unloaded to a state of zero stress, and then reloaded elastically in each of the coordinate directions to determine the reduced modulus of the material in each of the coordinate directions. From this data, the required damage parameters can be determined.

Failure Theory Overview

As discussed earlier in this paper, the majority of the available failure models utilize mathematical functions to describe the failure surface, which impose a specific shape on the failure surface. An example of this concept can be seen in Figure 1. In this figure, a two-dimensional failure surface in the σ_{11}-σ_{22} plane for the case of zero shear stresses generated using the two-dimensional version of the classical Tsai-Wu failure model for a representative AS4/3501-6 polymer matrix composite is shown. The properties used to generate the failure surface were taken from Daniel and Ishai [6]. Note that the actual failure surface is continuous but slight discontinuities are shown in the presented graphs due to numerical issues in the generation of the graph. As can be seen in the figure, the failure surface is elliptical due to the quadratic nature of the equation defining the failure surface. In reality, however, the failure surfaces of actual composites often do not exhibit this simple shape. Many actual failure surfaces cannot be easily defined by a mathematical function of the stresses. Alternatively, as shown in Figure 1, one potential method of defining the points in the failure surface is to use a cylindrical type of coordinate system. In this approach, a variable θ defines the relative location of the point on the failure surface in stress space, while a second variable r defines the "magnitude" of the failure surface point in the stress space location. Since the relationship between "r" and "θ" also cannot be easily defined by a mathematical function for a realistic composite failure surface, a tabulated approach, where a series of "r" and "θ" pairs are explicitly defined for a given failure surface, can provide a more accurate representation of the failure surface. The tabulated approach allows for the use of experimentally defined failure surface data, a

failure surface defined using any existing failure model, or a combination of experimental and numerically obtained "virtual" data. The combined approach can allow for the case where actual failure data are only available for a portion of the total stress space, with "virtual" data being required to fill in the gaps in the failure surface.
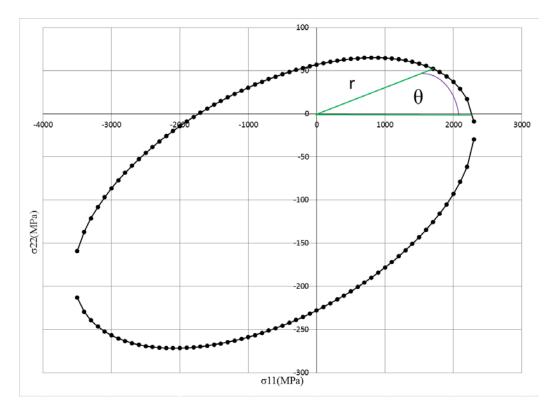

Figure 1: Tsai-Wu failure surface for AS4/3501-6 composite.

For the tabulated failure surface definition proposed in this study, appropriate independent and dependent variables need to be defined. The independent variables need to define the location of a point on the failure surface in stress space, and the dependent variable needs to define the magnitude of the failure surface point along the lines defined by the independent variables. For the current approach, the in-plane and out-of-plane responses will be considered separately. First, the definition of the in-plane failure surface will be discussed. For the in-plane failure surface definition, two independent variables are defined. The first independent variable will be the ratio of the shear stress to the shear failure stress. For selected values of this shear ratio, the location of each defined point on the failure surface in stress space is specified by defining the angle of the point in the σ_{11}-σ_{22} plane, as shown in Figure 1, which becomes the second independent variable. Using simple geometric principals, the angle θ for each defined point on the failure surface can be defined in terms of the stresses σ_{11} and σ_{22} as shown below. To ensure a set of unique, monotonically increasing angles from -180° to 180°, if the stress σ_{22} is negative the computed angle is multiplied by -1 as shown below:

$$\theta = \cos^{-1}\left(\frac{\sigma_{11}}{\sqrt{\sigma_{11}^2 + \sigma_{22}^2}}\right)$$

$$\theta_{act} = -\theta \ if \ \sigma_{22} \leq 0$$

(8)

For the dependent variable, which is used to define the magnitude of the failure surface point given a particular location in stress space, a stress invariant first identified by Fleischer et al [19] is used, defined as follows for the plane stress case:

$$r = \sqrt{\sigma_{11}^2 + \sigma_{22}^2 + 2\sigma_{12}^2}$$

(9)

This invariant can be considered to be like a "radius" from the origin to the failure surface. The factor of 2 in front of the shear stress term reflects the symmetry of the stress tensor. Stresses or strains can be used in defining the dependent variable, making the model more general. Using an invariant type of term also allows for the stress interactions to be more appropriately accounted for in the failure definition and helps to ensure that the failure definition will be accurate for a variety of loading conditions. One difficulty in using a tabulated approach of this type is that for many polymer matrix composites the failure surface is highly anisotropic due to the high failure strength in the fiber direction and the much lower failure stresses in the transverse direction. If one were to scale the y axis of the graph shown in Figure 1 such that it was equal to the scale of the x axis, one would observe that the actual failure surface is highly elongated. Due to the significant elongation of the failure surface, if one were to plot the radius versus the angle for the failure surface defined above, the majority of the points of the failure surface would be clustered at angles near -180°, 0°, and 180°. This clustering would create round-off and interpolation difficulties in the numerical implementation of the failure model, making the current definition undesirable.

To facilitate a more even distribution of the tabulated failure surface points along the entire spectrum of angles, the stresses used in the definition of the independent variable θ can be scaled. For the current method, the stresses in the 11-direction are arbitrarily scaled by the longitudinal tensile failure stress, and the 22-direction stresses are scaled by the transverse tensile failure stress. Revised angles are then computed using these scaled stresses. The value of the dependent variable *r*, however, is still computed using the actual unscaled stresses.

As mentioned earlier, for the proposed approach the procedure described above needs to be repeated for several ratios of the shear stress to the shear failure stress in order to fully define the in-plane failure surface. As failure surfaces similar to that shown in Figure 1 are generated with higher shear stress values, one can observe that increasing the shear stresses results in a failure surface with the same shape as the surface generated assuming zero shear stresses, but the location of the failure surface is shifted somewhat towards the negative stress quadrant of the graph. At high values of shear stresses, the failure surface may not even include the origin. Even when the origin is included, the fact that the failure surface is not centered on the origin may cause the angle calculations to be skewed. If the failure surface does not include the origin, the angle calculations would not even be valid as they would not be unique. To mitigate this issue, in the current approach the origin of the scaled failure surfaces for the selected shear stress ratios are redefined such that they lie in the center of the failure surface. The modified center of each failure surface is then defined based on the maximum and minimum scaled stress values in the 11- and 22-directions.

The angle calculations shown in Equation (8) are carried out using the revised stresses. The radius calculations are carried out using the original, unscaled and unmodified stresses. The radius versus scaled angle plot determined using the modified, scaled failure surface center is shown in Figure 2. As can be seen in the figure, the tabulated points defining the failure surface are evenly distributed across the range of angles. This data can easily be converted into a tabular format. In the numerical implementation of the theory, for a particular stress state the angle and radius can be computed. For the computed angle, if the radius is greater than the value of the radius at failure computed using the input failure data, the element is considered to have failed. Note that for the full three-dimensional case where out-of-plane stresses are significant, similar calculations can be made

using the out-of-plane stresses, and the interactions between the in-plane and out-of-plane stresses can be specified by a combination of the two radius functions.
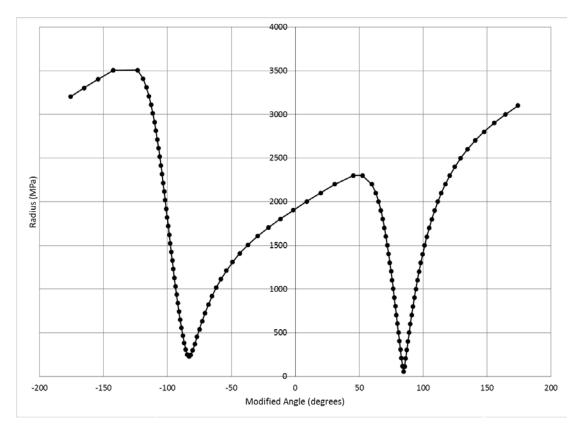

Figure 2. Plot of radius versus angle for scaled failure surface with modified center.

Verification and Validation Plan

A systematic verification and validation plan is currently being carried out to exercise the material model for a number of material system with varying fiber architectures, including unidirectional composites, weaves and tri-axial braids. First, a series of analyses are being carried out using a single element. The first step in the single element analysis process is to replicate the loading conditions that were used to provide the input data for the material model, specifically uniaxial tension curves in each of the normal directions (1,2,3), uniaxial compression curves in each of the normal directions (1,2,3), shear stress-strain curves in each of the shear directions (1-2, 2-3 and 3-1), and 45 degree off-axis tension or compression curves in each of the 1-2, 2-3 and 3-1 planes. By examining the results from these analyses, the ability of the code to accurately replicate the input data will be determined. By using single elements for this first set of verification and validation studies, complexities of the analysis caused by complicated boundary conditions, element interactions and edge effects can be avoided. In analyzing a realistic structure, simple loading conditions such as uniaxial tension are not present in every element in the finite element model. These simple single element analyses are the first step in assuring that the fundamental theory and numerical implementation of the code is correct, as a minimum requirement of a new material model should be that the input data can be replicated by analytical simulations. After the analyses of the single elements under simple loading are completed, the next step of the verification and validation process is to still analyze single elements, but to apply more complex loading conditions, such as combined tension and shear loadings, multiaxial tension or compression, and load/unload cycles. By conducting these analyses, constant, controlled load conditions are still applied to the element, but by applying

multiaxial loading the capability of the material model to properly account for all of the stress interactions can be examined. In this manner, the appropriateness of the theory and numerical implementation can be further verified. After the single element analyses are completed, the next step in the verification and validation process will be to explicitly model the coupon tests which were used to generate the input data for the particular material being simulated. By simulating the coupon tests, relatively simple loading conditions will still be applied to the finite element model, but the ability of the code to simulate structures under more realistic boundary conditions and stress/strain gradients will be determined. Finally, various flat and curved panel impact tests are being simulated in order to validate the ability of the code to predict the impact response of composite structures under realistic impact loading conditions. Since the material model was specifically designed to more accurately simulate the impact response of composites, the ability of the code to appropriately simulate the response of composite structures subject to realistic impact conditions is critical. All of these verification and validation efforts are ongoing and will be documented in future reports.

Acknowledgements

References

[1] Hallquist, J.: LS-DYNA Keyword User's Manual, Version 970. Livermore Software Technology Corporation, Livermore, CA, 2013.
[2] Matzenmiller, A.; Lubliner, J; and Taylor, R.L.: "A constitutive model for anisotropic damage in fiber-composites," *Mechanics of Materials*, Vol. 20, pp. 125-152, 1995.
[3] Sun, C.T.; and Chen, J.L.: "A Simple Flow Rule for Characterizing Nonlinear Behavior of Fiber Composites," *Journal of Composite Materials*, Vol. 23, pp. 1009-1020, 1989.
[4] Goldberg, R.; Carney, K.; DuBois, P.; Hoffarth, C.; Harrington, J.; Rajan, S.; and Blankenhorn, G: "Theoretical Development of an Orthotropic Elasto-Plastic Generalized Composite Model,", NASA/TM-2014-218347, National Aeronautics and Space Administration, Washington, D.C, 2014.
[5] Goldberg, R.; Carney, K.; DuBois, P.; Hoffarth, C.; Rajan, S.; and Blankenhorn, G: "Incorporation of Plasticity and Damage Into an Orthotropic Three-Dimensional Model With Tabulated Input Suitable for Use in Composite Impact Problems," NASA/TM-2015-218849, Washington, D.C., 2015.
[6] Daniel, I.M; and Ishai, O.: Engineering Mechanics of Composite Materials. Oxford University Press, New York, 2006.
[7] Hashin, Z.: "Failure Criteria for Unidirectional Fiber Composites." *J. Appl. Mech.*, Vol. 47, pp. 329-334, 1980.
[8] Puck, A.; and Schurmann, H.: "Failure Analysis of FRP Laminates by Means of Physically Based Phenomenological Models." *Composites Science and Technology*, Vol. 58, pp. 1045–1067, 1998.
[9] Pinho, S.T.; Iannucci, L.; Robinson, P.: "Physically-Based Failure Models and Criteria for Laminated Fibre-Reinforced Composites With Emphasis on Fibre Kinking: Part I: Development." *Composites: Part A*, Vol. 37 pp. 63-73, 2006.
[10] Maimi, P.; Camanho, P.P.; Mayugo, J.A.; and Davila, C.G.: "A Continuum Damage Model for Composite Laminates: Part I-Constitutive Model." *Mechanics of Materials*, Vol. 39, pp. 897-908, 2007.
[11] Mayes, J.S.; and Hansen, A.C.: "Multicontinuum Failure Analysis of Composite Structural Laminates." *Mech. Comp. Mat. Struct.*, Vol., 8, pp. 249-262, 2001.
[12] Feng, A.W.: "A Failure Criteria for Composite Materials." *Journal of Composite Materials*, Vol. 25, pp. 88-100, 1991.
[13] Hinton, M.J., and Kaddour, A.S.: "The background to the Second World-Wide Failure Exercise." *Journal of Composite Materials*, Vol. 46, pp. 2283-2294, 2012.
[14] Kaddour, A.S.; Hinton, M.J.; Smith, P.A.; and Lee, S.: "The background to the third world-wide failure exercise." *Journal of Composite Materials*, Vol. 47, pp. 2417-2426, 2013.
[15] Kaddour, A.S.; Hinton, M.J.; Smith, P.A.; and Lee, S.: "A comparison between the predictive capability of matrix cracking, damage and failure criteria for fibre reinforced composite laminates: Part A of the third world-wide failure exercise." *Journal of Composite Materials*, Vol. 47, pp. 2749-2779.
[16] Khan, A.S.; and Huang, S.: Continuum Theory of Plasticity. John Wiley and Sons, New York, 1995.
[17] Barbero, E.J.: Finite Element Analysis of Composite Materials Using ABAQUS. CRC Press, Boca Raton, FL, 2013.
[18] Lemaitre, J.; and Desmorat, R.: Engineering Damage Mechanics: Ductile, Creep and Brittle Failures. Springer, Berlin, 2005.
[19] Fleischer M.; Borrvall, T.; and Bletzinger, K.-U.: "Experience from using recently implemented enhancements for Material 36 in LS-DYNA 971 performing a virtual tensile test", 6th European LS-DYNA Users Conference, Gothenburg, Sweden, 2007..